Doubly-fed induction generator control via integral high order sliding modes

Héctor Huerta

Universidad de Guadalajara, Centro Universitario de los Valles,
Carretera Guadalajara - Ameca Km. 45.5, C.P. 46600, Ameca, Jalisco, México,
(e-mail: hector.huerta@profesores.valles.udg.mx).

Abstract: In this paper, the integral sliding modes with high order sliding modes is presented to control a wind energy conversion system, with a doubly-fed induction generator connected to a wind turbine. The mathematical model takes into account the dynamics of the generator, the wind turbine and the connections with the electrical network. The control objectives are the active power output and power factor regulation in the stator of the generator, which are achieved with the proposed controller without an extra control loop for the machine currents. An observer is not needed, since the control law depends on the terminal voltages and currents only that can be measured directly. A complete stability analysis of the closed-loop system is carried out. The effectiveness of the proposed controller was proved by simulations, in spite of perturbations.

Keywords: Nonlinear control systems, robust control, sliding mode control, wind energy, wind power generation.

1. INTRODUCTION

In order to decrease the greenhouse gas emissions due to the use of fossil fuels, the renewable energies have increased their importance, in particular, the wind energy. Indeed, several countries in the world have implemented huge wind farms (Burlibasa et al., 2012; Wang et al., 2012). In the case of wind turbines, the use of generators with constant speed could be difficult, due to the random behaviour of the wind. Then, the generators with variable speed could be better, and the Doubly-Fed Induction Generator (DFIG) have demonstrated its effectiveness. The DFIG is composed of two windings, one in the stator, connected directly to the electrical network, and the other in the rotor, connected to the electrical network through a bidirectional AC – AC power converter. The schematic diagram of the connection for the DFIG is shown in Fig. 1. The electronic power converter could have back-to-back or matrix topology. For the DFIG, the converter requires about the 20%-30% of the power output in the generator, which results in a little converter. Additionally, it is possible to regulate the active and reactive power in the generator, by using the power converter (Iacchetti et al., 2014).

On the other hand, in the Electric Power Systems (EPS) are several components, for example, generators, transmission lines, loads, etc. The EPS are subject to disturbances, such that parameter variations, programmed disconnection of elements and several faults, e. g., short circuits in lines, loads or generators (Kassem et al., 2013). The connection of the wind farms to the electrical network is needed, then, the DFIG is subject to the perturbations and nonlinearities of the complete EPS. In addition, the mechanical torque given by the wind turbine is time varying, since it depends on the wind conditions. Thus, the controller of the DFIG must take into account the previous conditions, including the rejection of perturbations, random behavior of the wind and nonlinear

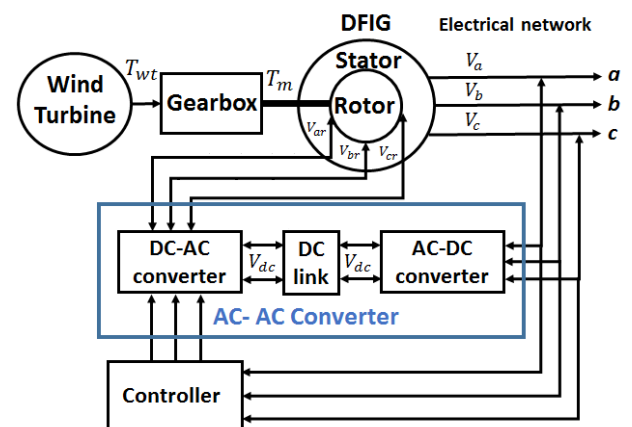region of operation, as well as offer robustness in all admissible operation points. (Jiabing and Yikang, 2009).

Fig. 1. Schematic diagram of the DFIG.

Although the DFIG in the wind farms has operated with controllers designed with linear techniques (Ghedamsi and Aouzellag, 2010; Mansour et al., 2011), these controllers could not guarantee a good performance, since they do not offer robustness due to the design depends on the plant parameters and are developed considering linear regions, tuned around a single equilibrium point (Zarei and Asaei, 2016). There are some techniques to improve the performance of the linear controllers, see for example (Zarei and Asaei, 2016; Javan et al., 2013). However, these controllers take into account a single operation point of the system again, so that they are limited to a small region of operation. To avoid the limitations of linear controllers, and take into consideration the complete nonlinear operation region of the DFIG, nonlinear controllers have been presented in the literature, for example passivity analysis (Song and Qu, 2013) and feedback linearization (Leon et al., 2012). Even though these nonlinear controllers could

improve the performance of linear controllers, they were designed considering the nominal plant parameters, which results in the lack of robustness, in spite of plant parameter variations. Some adaptive techniques, for example fuzzy logic (Jafari et al., 2014; Jazaeri and Samadi, 2015) and artificial neural networks (Marchi et al., 2014), could avoid the problems mentiones above, but the direct application of these techniques could produce a complicated algorithm with a high computational effort.

Furthermore, the Sliding Modes (SM) approach offers robustness under external disturbances and parameters variations in the plant. SM technique has demonstrated its effectiveness in electromechanical systems (Rossomando et al., 2014), renewable energy systems (Belkaid et al., 2016) and the DFIG (Abdeddaim and Betka, 2013; Patnaik et al., 2016). However, the direct implementation of sliding mode controllers to the DFIG would provoke finite-frequency, finite-amplitude oscillations (chattering), since the unmodeled fast electrical dynamics could be excited (Utkin et al., 1999). In order to avoid chattering and maintain the robustness with respect to matched perturbations with bounded and smooth control signals, alternative techniques based on SM can be applied, for example, the High Order Sliding Modes (HOSM) (Fridman and Levant, 1996; Moreno and Osorio, 2008). In (Morfin et al., 2014), the HOSM was presented, considering the block control feedback linearization and super-twisting algorithm, to regulate the electromagnetic torque and power factor in the stator. Nevertheless, the power output in the stator is not regulated and the sliding manifold could be difficult to design. In (Huerta, 2014) it was presented a HOSM controller for the DFIG, however, the turbine behavior was not considered and the robustness analysis was not included. Furthermore, in (Huerta, 2016), a passivity with sliding modes controller was presented, but the turbine behavior was omitted again and the solution converges to the sliding manifold asymptotically, instead of in a finite time.

Considering two control objectives, the active power output and Power Factor (PF) regulation in the stator of the DFIG, in this paper a novel control scheme is developed, specifically, Integral High Order Sliding Modes (IHOSM). A fifth order mathematical model is introduced, which takes into account the wind turbine and the interconnections to the EPS. The dynamics for the power output of the stator are obtained as well. In order to reject the internal perturbations and external disturbances since the first instant of time, the Integral Sliding Modes (ISM) approach is applied (Utkin et al., 1999). The ISM enables to reduce the computational effort and simplify the design of the sliding manifold that is used to stabilize the complete system. Then, a sliding manifold vector is chosen, to deal with the control objectives, in this case, the active power output and PF regulation in the stator of the DFIG, taking into account the stator power output unperturbed dynamics. The HOSM approach is considered, to induce the systems trajectories to the sliding manifolds vector and produce a smooth control signal, to avoid chattering. With the proposed control scheme, a control loop to regulate the currents in the stator is not needed, since the control law depends directly on the state vector. Furthermore, the

rejection of the matched perturbations can be accomplished, for example, external disturbances, such as short circuits, mechanical torque variations and voltage variations, and internal disturbances, like parameter variations in the system.

2. SYSTEM MODEL

The DFIG presented includes the mathematical description of the wind turbine and the mechanical, rotor and stator electrical dynamics. Then, based on the electrical dynamics, the active and active and reactive stator power output dynamics are developed.

2.1 DFIG electrical dynamics

Consider a balanced DFIG presented in the synchronous reference frame, that is, after the Park transformation. Taking into account the machine currents, the electrical dynamics can be presents as (Krause et al., 2002):

$$\frac{d}{dt}\boldsymbol{I}_{dq} = \boldsymbol{A}\boldsymbol{I}_{dq} + \boldsymbol{B}\boldsymbol{V}_{dq} + \boldsymbol{g}(\boldsymbol{I}_{dq}, \boldsymbol{V}_{dqs}, T_m) \qquad (1)$$

which can be witten as:

$$\begin{bmatrix} \frac{d}{dt}\boldsymbol{I}_{dqs} \\ \frac{d}{dt}\boldsymbol{I}_{dqr} \end{bmatrix} = \boldsymbol{A}\begin{bmatrix} \boldsymbol{I}_{dqs} \\ \boldsymbol{I}_{dqr} \end{bmatrix} + \boldsymbol{B}\begin{bmatrix} \boldsymbol{V}_{dqs} \\ \boldsymbol{V}_{dqr} \end{bmatrix} + \boldsymbol{g}(\boldsymbol{I}_{dq}, \boldsymbol{V}_{dqs}, T_m) \qquad (2)$$

where $\boldsymbol{I}_{dq} = \begin{bmatrix} \boldsymbol{I}_{dqs}\ \boldsymbol{I}_{dqr} \end{bmatrix}^T$ is the state vector, $\boldsymbol{I}_{dqs} = \begin{bmatrix} I_{ds}\ I_{qs} \end{bmatrix}^T$ is the stator currents vector, $\boldsymbol{I}_{dqr} = \begin{bmatrix} I_{dr}\ I_{qr} \end{bmatrix}^T$, is the rotor currents vector, $\boldsymbol{V}_{dq} = \begin{bmatrix} \boldsymbol{V}_{dqs}\ \boldsymbol{V}_{dqr} \end{bmatrix}^T$ is the input vector, $\boldsymbol{V}_{dqs} = \begin{bmatrix} V_{ds}\ V_{qs} \end{bmatrix}^T$ is the stator voltages vector and $\boldsymbol{V}_{dqr} = \begin{bmatrix} V_{dr}\ V_{qr} \end{bmatrix}^T$, is the rotor voltages vector. The perturbation term

$$\boldsymbol{g}(\boldsymbol{I}_{dq}, \boldsymbol{V}_{dq}, T_m) = \begin{bmatrix} \boldsymbol{g}_s(\boldsymbol{I}_{dq}, \boldsymbol{V}_{dqs}, T_m)\ \ \boldsymbol{g}_r(\boldsymbol{I}_{dq}, \boldsymbol{V}_{dqs}, T_m) \end{bmatrix}^T$$

includes external disturbances and parameter variations. Moreover:

$$\boldsymbol{A} = \begin{bmatrix} \boldsymbol{A}_{11} & \boldsymbol{A}_{12} \\ \boldsymbol{A}_{21} & \boldsymbol{A}_{22} \end{bmatrix}, \boldsymbol{B} = \begin{bmatrix} \boldsymbol{B}_{11} & \boldsymbol{B}_{12} \\ \boldsymbol{B}_{21} & \boldsymbol{B}_{22} \end{bmatrix},$$

$$\boldsymbol{A}_{11} = \begin{bmatrix} -\frac{r_s}{L_s\alpha} & \omega_s - \omega_r\frac{\alpha-1}{\alpha} \\ \omega_r\frac{\alpha-1}{\alpha} - \omega_s & -\frac{r_s}{L_s\alpha} \end{bmatrix}, \quad \boldsymbol{B}_{11} = \begin{bmatrix} -\frac{1}{L_s\alpha} & 0 \\ 0 & -\frac{1}{L_s\alpha} \end{bmatrix},$$

$$\boldsymbol{A}_{12} = \begin{bmatrix} -\frac{L_m r_r}{L_s L_r\alpha} & -\frac{L_m}{L_s\alpha}\omega_r \\ \frac{L_m}{L_s\alpha}\omega_r & -\frac{L_m r_r}{L_s L_r\alpha} \end{bmatrix}, \boldsymbol{B}_{12} = \begin{bmatrix} \frac{L_m}{L_s L_r\alpha} & 0 \\ 0 & \frac{L_m}{L_s L_r\alpha} \end{bmatrix},$$

$$\boldsymbol{A}_{21} = \begin{bmatrix} -\frac{L_m r_s}{L_s L_r\alpha} & \frac{L_m}{L_r\alpha}\omega_r \\ -\frac{L_m}{L_r\alpha}\omega_r & -\frac{L_m r_s}{L_s L_r\alpha} \end{bmatrix}, \boldsymbol{B}_{21} = \begin{bmatrix} -\frac{L_m}{L_s L_r\alpha} & 0 \\ 0 & -\frac{L_m}{L_s L_r\alpha} \end{bmatrix},$$

$$\boldsymbol{A}_{22} = \begin{bmatrix} -\frac{r_r}{L_r\alpha} & \omega_s - \omega_r\frac{1}{\alpha} \\ \omega_r\frac{1}{\alpha} - \omega_s & -\frac{r_r}{L_r\alpha} \end{bmatrix}, \boldsymbol{B}_{22} = \begin{bmatrix} -\frac{1}{L_r\alpha} & 0 \\ 0 & \frac{1}{L_r\alpha} \end{bmatrix},$$

$$\alpha = 1 - \frac{L_m^2}{L_s L_r}.$$

Furthermore, $L_m = \frac{x_m}{\omega_b}$, $L_s = \frac{x_{ls}}{\omega_b} + L_m$ and $L_r = \frac{x_{lr}}{\omega_b} + L_m$.

Remark 1. It is important to note that the perturbations vector $\boldsymbol{g}(\boldsymbol{I}_{dq}, \boldsymbol{V}_{dq}, T_m)$ can include several disturbances, for example parameter variations, mechanical torque variations and interconnection voltage variations (Javan et al., 2013).

Remark 2. Due to the interconnection of the DFIG with the electrical network, the terminal voltage of the generator can be considered constant, so that $\boldsymbol{V}_{dqs}$ is presented as a vector with constant value elements. Then, the control input for the DFIG is the rotor voltages vector $\boldsymbol{V}_{dqr}$.

2.2 DFIG mechanical dynamics

Taking into account the wind speed, v_w, the mechanical power output of a wind turbine can be expressed as (Rahim and Habiballah, 2011)

$$P_{wt} = \frac{1}{2} \rho \pi R^2 C_p(\gamma, \beta) v_w^3 \tag{3}$$

where ρ is the air density, R is the rotor diameter and $C_p(\gamma, \beta)$ is the power coefficient that represents the efficiency of the blades at the operation point. Considering a wind turbine with three blades it follows that $0.25 < C_p < 0.45$ and it can be approximated as (Hachicha and Krichen, 2012)

$$C_p(\gamma, \beta) =$$
$$0.73 \left(\frac{151}{\gamma_i} - 0.58\beta - 0.002\beta^{2.14} - 13.2 \right) e^{\frac{-18.4}{\gamma_i}} \tag{4}$$

β is the blade tip pitch angle, γ is the tip speed ratio, presented as:

$$\gamma = \frac{R\omega_t}{v_w} \tag{5}$$

ω_t is the wind turbine rotational speed. From (3) – (6) it follows:

$$\gamma_i = \left(\frac{1}{\gamma - 0.02\beta} - \frac{0.003}{\beta^3 + 1} \right)^{-1} \tag{6}$$

The wind speed varies randomly all day. Nevertheless, the average wind speed can be considered as a constant value in some intervals of time. Then, the variations of the wind speed, can be presented as a linear combination of the constant wind speed, and sinusoidal variations (Datta and Ranganathan, 2002):

$$v_w = v_m \left[1 - 0.2cos\left(\frac{2\pi t}{20} \right) - 0.5cos\left(\frac{2\pi t}{600} \right) \right] \tag{7}$$

where v_m is a constant wind speed. Then, changing the value v_m and the frequency of the sinusoidal variations, a wind gust could be obtained. The mechanical torque in the rotor of the wind turbine can be computed as

$$T_{wt} = \frac{P_{wt}}{\omega_t} \tag{8}$$

Furthermore, the mechanical torque in the rotor of the DFIG, T_m, is obtained from the wind turbine through a gearbox. The mechanical torque and rotor speed, ω_r, are calculated as follows

$$\omega_r = G\omega_t \tag{9}$$

$$T_m = \frac{T_{wt}}{G} \tag{10}$$

where G is the transmission rate. Finally, according to (Krause et al., 2002) the DFIG swing equation is written as

$$\frac{d}{dt}\omega_r = \frac{n_p}{2J_m}(T_m - T_e) \tag{11}$$

J_m is the constant of inertia, n_p is the number of poles of the DFIG and T_e is the electromagnetical torque in the generator, which is expressed as a function of the rotor and stator currents as follows:

$$T_e = \frac{3}{2} L_m \left(I_{qs} I_{dr} - I_{ds} I_{qr} \right) \tag{12}$$

Remark 3. It is worth mentioning that the DFIG model (1) - (12) is presented as a nonlinear model due to the swing equation in which the electromagnetical torque is given by (12) (Krause et al., 2002).

Finally, the DFIG state space model given by (1) - (12) will be used in the next section to obtain the dynamics of the active and reactive power in the stator.

2.3 Stator active and reactive power dynamics

Since the control objectives are the output active power and PF in the stator, it is necessary to obtain the dynamics of the stator output power. In this way it is possible to avoid an extra control loop for the rotor currents. Then, the stator active and reactive power in terms of the DFIG currents and voltages can be written as

$$\boldsymbol{PQ} = \boldsymbol{V}\boldsymbol{I}_{dqs} \tag{13}$$

where $\boldsymbol{PQ} = [P \ \ Q]^T$ is the stator active power output vector and

$$\boldsymbol{V} = \frac{3}{2} \begin{bmatrix} V_{ds} & V_{qs} \\ V_{qs} & -V_{ds} \end{bmatrix}.$$

Then, considering the DFIG electrical dynamics, (2), the time derivative of (13) becomes to:

$$\dot{\boldsymbol{PQ}} = \boldsymbol{f}_{PQ}(\boldsymbol{I}_{dq}, \boldsymbol{V}_{dqs}) + \boldsymbol{B}_{PQ}\boldsymbol{V}_{dqr} + \boldsymbol{g}_s(\boldsymbol{I}_{dq}, \boldsymbol{V}_{dqs}, T_m) \tag{14}$$

Where the elements of the vector $\boldsymbol{f}_{PQ}(\boldsymbol{I}_{dq}, \boldsymbol{V}_{dqs}) = \boldsymbol{V}(\boldsymbol{A}_{11}\boldsymbol{I}_{dqs} + \boldsymbol{A}_{12}\boldsymbol{I}_{dqr} + \boldsymbol{B}_{11}\boldsymbol{V}_{dqs})$ are continuous functions of time and $\boldsymbol{B}_{PQ} = \boldsymbol{V}\boldsymbol{B}_{12}$ is a nonsingular matrix with constant elements. Moreover, the vector of perturbations terms in the stator $\boldsymbol{g}_s(\cdot)$ includes parameters variations and external disturbances.

3. IHOSM CONTROL SCHEME

In this section the design of the IHOSM control scheme is presented, for the DFIG. A DFIG driven by a wind turbine is presented in Fig. 1. The machine has two windings, the stator winding is connected to the EPS, through the electrical grid, while the rotor winding needs an AC – AC electronic power converter, composed of two interconnected circuits, namely, the rotor side converter and grid side converter. The proposed control objectives can be achieved by means of the rotor side converter. The grid side converter is able to control the DC link voltage between the two converters, as well as the reactive power to the network. The DFIG can operate in a band of $\pm\Delta\omega_r$ around the synchronous speed, ω_s. When the rotor speed is greater than the synchronous speed, that is, $\omega_r > \omega_s$, the DFIG works in super - synchronous mode and the power is delivered to the electrical network from both, rotor and stator windings. On the other hand, when $\omega_r < \omega_s$ the DFIG is running in sub–synchronous mode, only the stator windings provides electrical power to the network, and

the power converter is fed from the electrical network to supply the rotor winding.

In this paper the grid side control is outlined. The control inputs to the system are the rotor voltages, V_{dr} and V_{qr}. Having two control inputs, it is possible to consider two control objectives, the active power output and PF regulation in the stator of the machine. At first, based on the difference between the stator active and reactive power output and their references values, the control error dynamics vector is obtained. Then, the ISM technique is applied to achieve an unperturbed error system. Finally, the sliding manifold vector for the HOSM controller is designed and implemented in a super twisting algorithm.

Before the introduction of the proposed IHOSM control scheme an important definition is stated:

Definition 1. Robust stabilization. Let the nonlinear system:

$$\dot{x} = f(x) + b(x)u + g(x,t) \tag{15}$$

where $x(t)$ is the state vector, $f(x)$ and $b(x)$ are smooth vector-fields, and $g(x,t)$ is the perturbation vector. The system (15) achieves robust stability if it is stable in the Lyapunov sense for all admissible perturbations Khalil, 1996).

It is important to note that the proposed IHOSM control scheme is robust according to the *Definition 1*, as it will be shown later.

3.1 IHOSM control scheme design

Given the control objectives, from the active power output and Power Factor (PF) regulation in the stator of the DFIG, a reference values vector is presented. Considering the active and reactive power output in the stator, the PF can be expressed as follows:

$$PF = \frac{P}{\sqrt{P^2+Q^2}} \tag{16}$$

Solving (16) for the reactive power, its reference value, Q_{ref}, is written as:

$$Q_{ref} = P_{ref}\sqrt{\frac{1}{PF_{ref}} - 1} \tag{17}$$

Then, the control error vector, e, is defined as the difference between the stator power output vector, PQ, and the reference values vector, PQ_{ref}, i. e.

$$e = PQ - PQ_{ref} \tag{18}$$

where $PQ_{ref} = \begin{bmatrix} P_{ref} & Q_{ref} \end{bmatrix}^T$. From the stator power output dynamics, (14), it is possible to obtain the time derivative of the control error vector (18), as follows:

$$\dot{e} = f_{PQ}(I_{dq}, V_{dqs}) + g_{PQ}(I_{dq}, V_{dqs}, T_m) + B_{PQ}V_{dqr} \tag{19}$$

where $g_{PQ}(I_{dq}, V_{dqs}, T_m) = g_s(I_{dq}, V_{dqs}, T_m) - \dot{P}Q_{ref}$, is the perturbations term, that contains internal disturbances and external perturbations.

It is worth mentioning that the following assumptions must be considered in the control scheme design procedure of the IHOSM:

A1. The perturbation term, $g_{PQ}(I_{dq}, V_{dqs}, T_m)$, in (11) satisfies the matching condition, that is, there exists the vector $\bar{g}$ such that (Utkin et al., 1999)

$$g_{PQ}(I_{dq}, V_{dqs}, T_m) = B_{PQ}\bar{g} \tag{20}$$

A.2. The perturbation term $g_{PQ}(I_{dq}, V_{dqs}, T_m)$ in (11) is bounded, i. e.:

$$\left| g_{PQ}(I_{dq}, V_{dqs}, T_m) \right| \le g_{PQ}^+(t).$$

A.3. The nominal parameters of the DFIG mathematical model (1) - (12) are known.

A.4. The mechanical torque input in (11) is assumed as a slow varying and bounded function of time.

It is important to note that the proposed control scheme differs from the classical sliding mode approach, since a hyperbolic tangent function, $tanh(x)$, is applied instead of the $sign(x)$ function. This is possible, due to (Castillo et al., 2007)

$$lim_{\varepsilon \to 0} tanh\left(\frac{x}{\varepsilon}\right) = sign(x), \ \varepsilon \in \mathbb{R}^+ \tag{21}$$

Next, in order to reject the perturbation term $g_{PQ}(I_{dq}, V_{dqs}, T_m)$ in (19), since the first instant of time, the ISM technique will be applied. Then, the HOSM with a super twisting algorithm will be used in the unperturbed system.

Thus, according to the ISM technique (Utkin et al., 1999), defining the control input V_{dqr} in the control error dynamics given by (19) as:

$$V_{dqr} = V_{dqr,0} + V_{dqr,1} \tag{22}$$

it follows

$$\dot{e} = f_{PQ}(I_{dq}, V_{dqs}) + g_{PQ}(I_{dq}, V_{dqs}, T_m) + B_{PQ}V_{dqr,0} + B_{PQ}V_{dqr,1} \tag{23}$$

where $V_{dqr,0}$, the first part of the control input, is designed to stabilize the DFIG around its equilibrium point and add damping, in spite of perturbations. $V_{dqr,1}$, the second part of the control input, is selected to reject the perturbation term $g_{PQ}(I_{dq}, V_{dqs}, T_m)$. According to the ISM technique, to design the second part of the control input, $V_{dqr,1}$, a sliding manifold vector is stablished as

$$s_1 = e + \sigma \tag{24}$$

where $s_1 = [s_{11} \ s_{12}]^T$ and $\sigma = [\sigma_1 \ \sigma_2]^T$ is the integral variables vector. Taking into account (23), the time derivative of the sliding manifold vector s_1, (24), can be presented as:

$$\dot{s}_1 = f_{PQ}(I_{dq}, V_{dqs}) + g_{PQ}(I_{dq}, V_{dqs}, T_m) + B_{PQ}V_{dqr,0} + B_{PQ}V_{dqr,1} + \dot{\sigma} \tag{25}$$

Then, from (25), the dynamics for the integral variables vector $\dot{\sigma}$ are selected as

$$\dot{\sigma} = -\boldsymbol{f}_{PQ}(\boldsymbol{I}_{dq}, \boldsymbol{V}_{dqs}) - \boldsymbol{B}_{PQ}\boldsymbol{V}_{dqr,0}, \sigma(0) = -\boldsymbol{e}(0) \qquad (26)$$

Moreover, considering (26) and the matching condition defined in the assumption *A.1*, equation (20), the dynamics for the sliding manifold vector $\dot{\boldsymbol{s}}_1$ (25) becomes to

$$\dot{\boldsymbol{s}}_1 = \boldsymbol{B}_{PQ}(\overline{\boldsymbol{g}} + \boldsymbol{V}_{dqr,1}) \qquad (27)$$

Then, select $\boldsymbol{V}_{dqr,1}$ in (25) as

$$\boldsymbol{V}_{dqr,1} = -k_1 tanh(\boldsymbol{s}_1) \qquad (28)$$

where $tanh(\boldsymbol{s}_1) = [tanh(s_{11}) \ tanh(s_{12})]^T$, and $k_1 \in \mathbb{R}^+$. Considering (26) and (27), under the condition

$$k_1 > |\overline{\boldsymbol{g}}| \qquad (29)$$

the trajectories of (25) tends to the sliding manifold $s_1 = 0$, (24), (Castillo et al., 2007). The sliding mode motion is governed by

$$\dot{\boldsymbol{e}} = \boldsymbol{f}_{PQ}(\boldsymbol{I}_{dq}, \boldsymbol{V}_{dqs}) + \boldsymbol{B}_{PQ}(\overline{\boldsymbol{g}} + \boldsymbol{V}_{dqr,1eq}) + \boldsymbol{B}_{PQ}\boldsymbol{V}_{dqr,0},$$

where $\boldsymbol{V}_{dqr,1eq}$ is the equivalent control obtained with $\dot{\boldsymbol{s}}_0 = 0$, (27), that can be written as $\boldsymbol{V}_{dqr,0eq} = \overline{\boldsymbol{g}}$. Therefore, the equivalent control $\boldsymbol{V}_{dqr,1eq}$ reject the perturbation term $\boldsymbol{g}_{PQ}(\boldsymbol{I}_{dq}, \boldsymbol{V}_{dqs}, T_m)$ in (23). Moreover, as the Integral Sliding Modes stated, chosing $\boldsymbol{\sigma}(0) = -\boldsymbol{e}(0)$, the perturbation vector is rejected since the first instant of time (Utkin et al., 1999), and the sliding mode equation to represent the control error $\boldsymbol{e}$ is written as an unperturbed system:

$$\dot{\boldsymbol{e}} = \boldsymbol{f}_{PQ}(\boldsymbol{I}_{dq}, \boldsymbol{V}_{dqs}) + \boldsymbol{B}_{PQ}\boldsymbol{V}_{dqr,0} \qquad (30)$$

In order to design the second part of the control input (22), $\boldsymbol{V}_{dqr,0}$, the HOSM technique is applied, by using the super twisting algorithm. Then, the sliding manifold vector $\boldsymbol{s}_0 = [s_{01} \ s_{02}]^T$ is presented, as the control error vector, that is

$$\boldsymbol{s}_0 = \boldsymbol{e} \qquad (31)$$

Then, according to the super twisting algorithm (Fridman and Levant, 1996), it follows:

$$\boldsymbol{V}_{dqr,0} = -k_{0,1}\sqrt{\|\boldsymbol{s}_0\|}tanh(\boldsymbol{s}_0) + \boldsymbol{u},$$
$$\dot{\boldsymbol{u}} = -k_{0,2}tanh(\boldsymbol{s}_0) \qquad (32)$$

where $k_{0,1}, k_{0,2} \in \mathbb{R}^+$. Under the conditions $k_{0,1} > 0$ and $k_{0,2} > 0$, the solution of the closed-loop system (30) with (32) reaches the sliding manifold $\boldsymbol{s}_0 = 0$ in a finite time (Moreno and Osorio, 2008) and the control error vector $\boldsymbol{e}$ tends exponentially to zero.

It is worth mentioning that selecting $\boldsymbol{V}_{dqr,0}$ as in (32), the attractiveness of the sliding manifold (31) is guaranteed, achieving the both control objectives, in this case, the active power output and PF regulation in the stator of the machine. Moreover, the control signal is bounded and smooth, avoiding chattering.

Remark 4. Two sliding manifolds are needed to complete the proposed control scheme. At first, $\boldsymbol{s}_0$ in $\boldsymbol{V}_{dqr,0}$ to guarantee the stability of the closed - loop system, and, secondly, $\boldsymbol{s}_1$ in

the second part of the control input, $\boldsymbol{V}_{dqr,1}$, to reject the perturbation term since the first instant of time.

Remark 5: In the case of the electric power systems, the steady-state initial values for the state vector are computed considering a pre-fault flow analysis, as in (Anderson and Fouad, 1994). Then, it is possible to obtain the initial conditions for the integral variables vector as $\boldsymbol{\sigma}(0) = -\boldsymbol{e}(0)$, required in (26).

3.2 IHOSM proposed controller main features

It is worth mentioning that there are some important remarks about the IHOSM proposed control scheme for the DFIG:

a) Both control objectives are fulfilled by obtaining the control error dynamics (19), which depends on the stator currents. So, it is not necessary the use of an extra control loop for the stator currents due to the sliding manifolds is presented as a function of the machine currents and voltages. Therefore, the proposed control scheme can be implemented directly with the measurements of these variables. Moreover, an observer is not needed.

b) Given the condition (29) for k_1, it is possible to reject all unknown matched perturbations that satisfy that bound, by means of the ISM controller, obtaining the robust stability, according to *Definition 1*. Examples of perturbations are mechanical torque variation due to the wind turbine, parameter variations in the system, rotor speed variations, changes in the EPS configuration, etc.

c) The effect of the complete EPS and its elements, including generators, transmission lines and loads, etc., are considered as variations in the interconnection voltages, $\boldsymbol{V}_{dqs}$, so that, they are contained in the perturbation term $\boldsymbol{g}_{PQ}(\boldsymbol{I}_{dq}, \boldsymbol{V}_{dqs}, T_m)$, in (19). In this way, the proposed IHOSM control scheme is able to reject the perturbations, providing the robust stabilization around the equilibrium point. Since the DFIG is connected to the EPS by the interconnection voltage only, it is possible to apply the proposed control scheme to any EPS, with *n* generators, *m* buses and *k* loads.

d) The proposed IHOSM control scheme enables to reject perturbations since the first instant of time due to are included the ISM and HOSM techniques. This can be done by the first part of the control law, (28). Furthermore, the chattering provoked by the fast electrical dynamics, is avoided by the inclusion of the second part of the control law (32). Two sliding manifold vectors were presented. The sliding manifold vector, $\boldsymbol{s}_1$, was chosen at first, to add robustness and reject the perturbation term $\boldsymbol{g}_{PQ}(\boldsymbol{I}_{dq}, \boldsymbol{V}_{dqs}, T_m)$ in (19). Then, the second sliding manifold vector $\boldsymbol{s}_0$ was selected to guarantee the system stabilization and achieve the both control objectives.

e) In general the sliding modes technique uses the $sign(\cdot)$ function in the control laws. In this work this function is replaced by a $tanh(\cdot)$ function. This change enables to decrease the undesirable high frequency commutation in the control inputs and system outputs, which are required in the implementation of the controller.

3.3. IHOSM proposed controller, practical issues.

Finally, a schematic diagram for the proposed controller implementation is presented in Fig. 2, where the DFIG and its interconnections with the IHOSM controller and other elements can be found. The wind turbine supplies the mechanical torque to the DFIG through a gearbox. The stator winding is connected directly to the EPS. The AC – AC power converter is a bidirectional electronic circuit to manage the power flow between the rotor and the EPS, and two topologies could be considered, a back-to-back or a matrix converter (Krause et al., 2002). The power converter feeds the rotor windings and takes the energy required from the electrical network.

Since the proposed controller is presented in the *dq0* reference frame, an *abc-dq0* transformation block is required. A PLL oscillator computes the stator angle which is needed by the transformation block. The stator currents and voltages in the *dq0* frame, i., I_{ds}, I_{qs}, V_{ds} and V_{qs}, and the DFIG rotor speed, measured directly from the machine shaft, are taken by the controller. Then, the IHOSM compute the corresponding rotor voltages, V_{dr} and V_{qr}, depending on the references values for the active power output and PF in the stator, as well as the DFIG operation conditions. Moreover, the rotor voltages are sent to another transformation block, that produce the rotor voltages in the *abc* frame, taking into account the stator angle, given by the PLL oscillator. Finally, the rotor voltages are sent to the AC- AC power converter to feed the rotor winding.

It is worth mentioning that the proposed IHOSM control scheme needs the DFIG rotor speed, as well as the stator voltages and currents. These signals are measured directly from the generator, in such a way that an observer is not required.
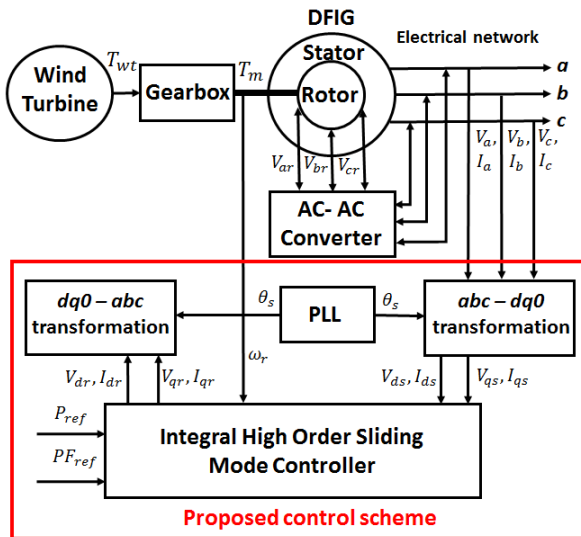

Fig. 2. Proposed control scheme diagram of the DFIG.

4. CASE STUDIES

In order to show the effectiveness of the proposed IHOSM control scheme the closed-loop (19) with (22) was tested by simulations. The reference values were selected as $P_{ref} =$

$600kW$ and $PF_{ref} = 0.95$. The DFIG parameters are $X_s = 8.8\Omega$, $X_r = 8.8\Omega$, $X_m = 180\Omega$, $r_s = 12.5\Omega$, $r_r = 3.9\Omega$, $P = 2$, $J_m = 0.0024kgm^2$, with rated voltage of 1.5kV. The simulations were carried out by using Simulink of MATLAB. The mathematical model and the control scheme were programmed directly as a functions. Moreover, a fixed integration step was included to cover the requirements of the real-time implementation of the sliding modes controller.

In Fig. 3-14 is presented the performance of the stator active power output and PF with the proposed IHOSM control scheme and a PI scheme, as well as the sliding manifolds convergence, with four different perturbations. The parameters of the control scheme were tuned as $k_{0,1} = 200$, $k_{0,1} = 150$ and $k_{0,2} = 0.5$ in the four cases. Moreover, since it is possible to calculate the steady-state values for the DFIG, as it was mentioned in *Section 3.1*, these values were set to the the closed-loop system in the case studies. The PI controller was tuned according to (Lee *at al.*, 2010).The four perturbations are described as follows:

a) In order to prove the PHOSM effectiveness under abruptly variations of parameters, the parameter L_m was incremented 50%, as an internal disturbance, in $t = 1s$. This kind of perturbations are produced by increments or decrements of the parameters nominal values, as a consequence of damage in the machine windings and/or mismatching in the nominal values. From (6) the perturbation term $g_{PQ}(\cdot)$ is computed as

$$g_{PQ}(I_{dq}, V_{dqs}, T_m) = V(\Delta A_{11}I_{dqr} + \Delta A_{12}I_{dqr} + \Delta B_{12}V_{dqr}) \tag{33}$$

where

$$\Delta A_{11} = \begin{bmatrix} -\dfrac{r_s}{L_S\Delta\alpha} & \omega_s - \omega_r\dfrac{\Delta\alpha-1}{\Delta\alpha} \\ \omega_r\dfrac{\Delta\alpha-1}{\alpha} - \omega_s & -\dfrac{r_s}{L_S\Delta\alpha} \end{bmatrix},$$

$\Delta\alpha = 1 - 0.25\dfrac{L_m^2}{L_sL_r}$, $\Delta A_{12} = 0.5A_{12}$ and $\Delta B_{12} = 0.5B_{12}$.

Defining

$$\bar{g} = B_{PQ}^{-1}g_{PQ}(I_{dq}, V_{dqs}, T_m) \tag{34}$$

the perturbation term (33) satisfies (20). In addition, the elements of the matrices A_{12} and B_{12} are bounded and the elements of the matrix V and the vectors I_{dqr} and V_{dqr} are bounded too. Then, the assumptions *A1* and *A2* are fulfilled.

b) Due to the mechanical torque, T_m, depends on the wind speed and density and, in general, these parameters varies randomly all day, the mechanical torque varies randomly too. Then, the second perturbation tested at $t = 1s$, to the closed-loop system, was a random variation of ±20% in the wind speed, around its initial value, producing a random mechanical torque variation. In this case, the perturbation term is given by:

$$g_{PQ}(I_{dq}, V_{dqs}, T_m) = \Delta A_{11}I_{dqs} + \Delta A_{12}I_{dqr} \tag{35}$$

where

$$\Delta A_{11} = \begin{bmatrix} 0 & -\Delta\omega_r \frac{\alpha-1}{\alpha} \\ \Delta\omega_r \frac{\alpha-1}{\alpha} & 0 \end{bmatrix},$$

$$\Delta A_{11} = \begin{bmatrix} 0 & -\Delta\omega_r \frac{L_m}{L_s\alpha} \\ \Delta\omega_r \frac{L_m}{L_s\alpha} & 0 \end{bmatrix},$$

and $\Delta\omega_r$ is an increment of the rotor speed due to the variation of the mechanical torque, T_m, in (11). Furthermore, equation (35) satisfies (20) with

$$\bar{g} = B_{PQ}^{-1}\left(\Delta A_{11}I_{dqs} + \Delta A_{12}I_{dqr}\right) \tag{36}$$

Again, the elements of the matrices ΔA_{11} and ΔA_{12} are bounded and the vectors I_{dqr} and I_{dqs} are bounded as well, then, the assumptions *A1* and *A2* are fulfilled.

c) The interconnection voltage was decremented by 50%, at $t = 1s$. The perturbation term is calculated as:

$$g_{PQ}\left(I_{dq}, V_{dqs}, T_m\right) = -0.5VB_{11}V_{dqs} \tag{37}$$

In order to satisfy (19), consider

$$\bar{g} = -0.5B_{PQ}^{-1}\left(VB_{11}V_{dqs}\right) \tag{38}$$

Additionally, due to the boundedness of the matrices B_{PQ}, V, and B_{11} and the vector V_{dqs}, the assumption *A1* is fulfilled.

d) The fourth perturbation corresponds to a three phase short circuit in terminals of the DFIG. This is a critical fault, was applied at $t = 1\ s$ and was cleared by setting the terminal voltages at their initial values at $t = 1.1\ s$. The fulfillment of assumptions can be carried out as in perturbation c.

It is important to note that according to (29), under the condition $k_1 > |\bar{g}|$, the four perturbations presented can be rejected by the ISM, where $\bar{g}$ can be calculated as in (34), (36) and (38).

Some important features are underlined about the performance of the closed – loop system (19) with the proposed IHOSM control scheme (22):

a) The both control objectives, in this case, the active power output and PF in the stator of the DFIG, are accomplished by the proposed IHOSM control scheme, in less than 0.5 s, in spite of perturbations.

b) The proposed IHOSM control scheme is able to stabilize the closed-loop system, in spite of small disturbances, e. g., parameter variations, and large disturbances, for example, mechanical torque variations, interconnection voltage variations and short circuits.

c) In the case of the transient performance, the closed-loop system (19) with (22) does not presents oscillations or overshoot after the fault, which shows the damping added to the system. On the other hand, a classical controller, e. g., a PI controller, presents several oscillations. This fact show the damping adding to the closed-loop system.

d) Perturbation b) shows that the proposed IHOSM is able to reject external disturbances, e. g., mechanical torque

variations, see in Fig. 6-8. When the wind speed varies randomly around its initial value the mechanical torque too, the response with the IHOSM control scheme varies around the active power output and PF references values, in a band of 0.3%. With the PI, the both responses tend to oscillate in a similar band but the stator active power output, as well as PF, tends to decrease their values.
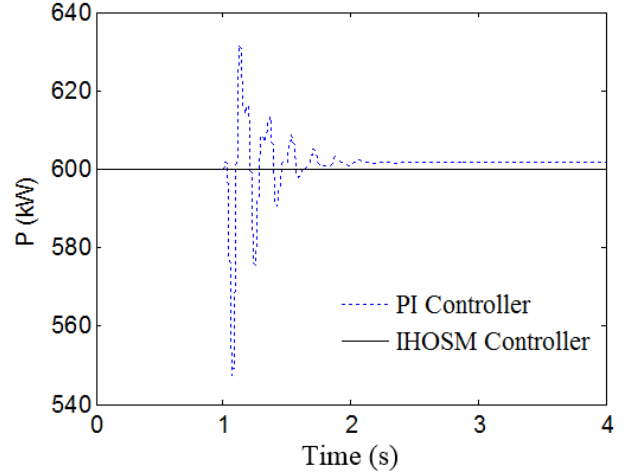

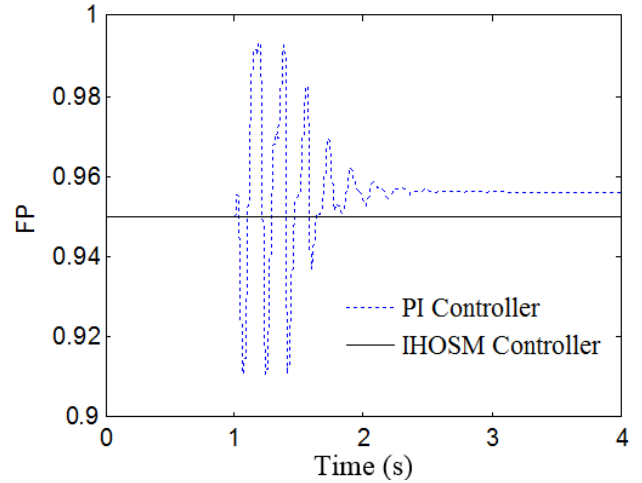Fig. 3. Stator active power under perturbation a).

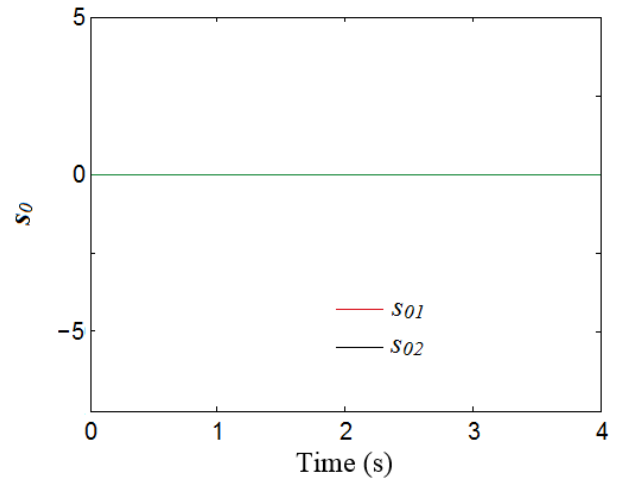Fig. 4. Power factor under perturbation a).

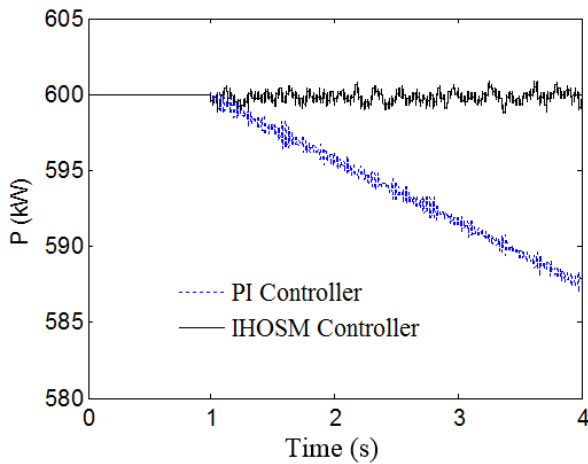Fig. 5. Sliding manifold convergence under perturbation a).
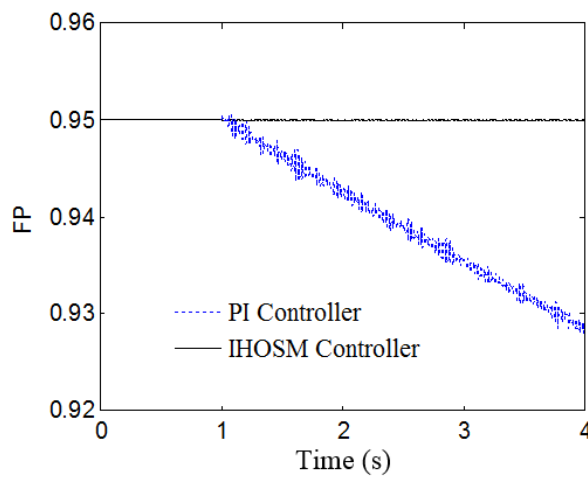
Fig. 6. Stator active power under perturbation b).

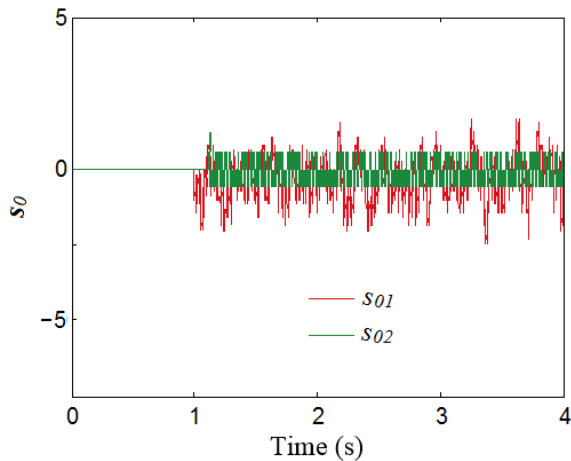Fig. 7. Power factor under perturbation b).

Fig. 8. Sliding manifold convergence under perturbation b).

e) The robustness of the IHOSM control scheme with respect to changes in the EPS configuration is shown with the perturbation *c)*, changing the interconnection voltage. In Fig. 9-11 are shown the result for this perturbation, in the stator active power the value increments but returns to its reference value with a maximum of about 11%. The PF present an increment of 0.2% and the final value is the same as the initial value. On the other hand, the response with the PI controller presents oscillations in both

responses, with an overshoot of 30% in the stator power output, moreover, the final values are different form the reference values after the introduction of the perturbation.
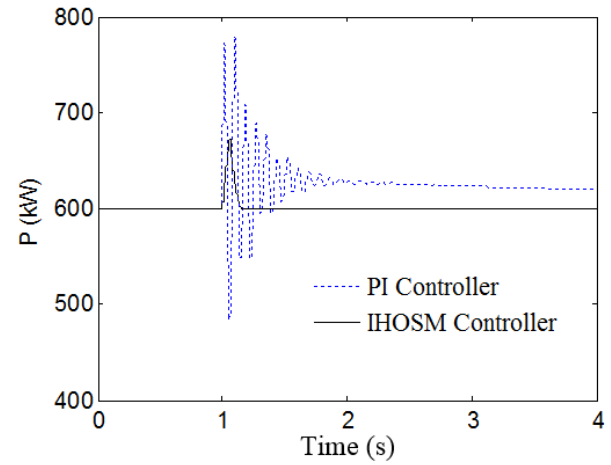

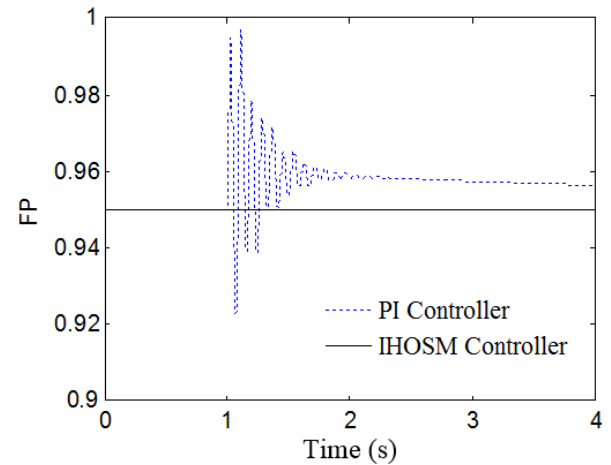Fig. 9. Stator active power under perturbation c).

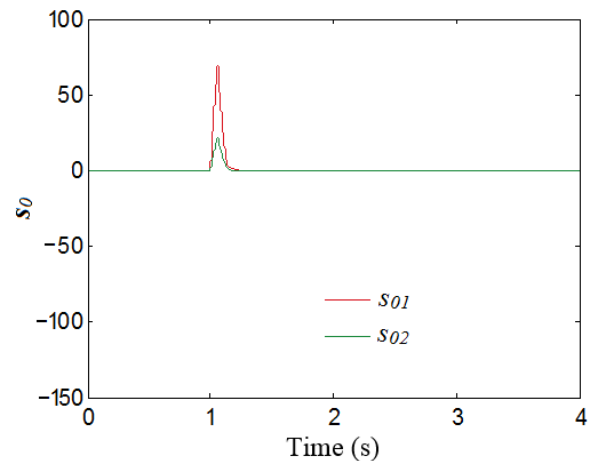Fig. 10. Power factor under perturbation c).

Fig. 11. Sliding manifold convergence under perturbation c).

f) The perturbation *d)* was considered to test the proposed IHOSM performance under critical faults, for example, a three phase short circuit in terminals of the DFIG. The responses with the proposed IHOSM present a similar behavior like in the perturbation *c)*. In this case the stator

active power and PF decrease their values but recover their respective reference values. Again, the responses with the PI controller presents oscillations and the steady state values are different form the reference values after the perturbation, see Fig. 12-14.

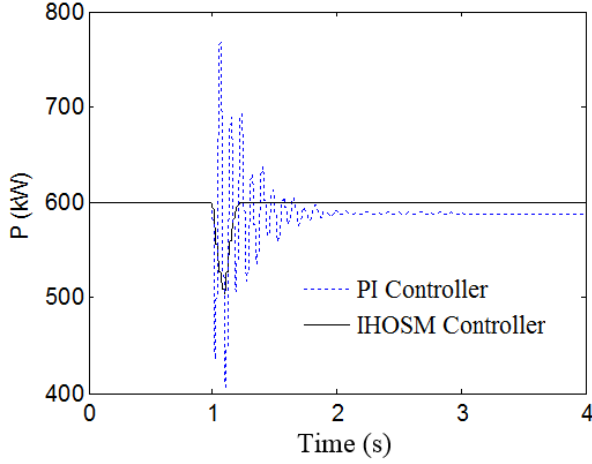g) In the four perturbations presented, the performance of the proposed IHOSM control scheme tends to be unaffected.

Fig. 12. Stator active power under perturbation d).

Remark 6. In case of a critical fault in the electrical network that could provoke the activation of a crowbar protection circuit, as a consequence, the active and reactive power are not demanded from the EPS. Then, the references for active and reactive power output in the DFIG must be set to zero in the implementation of the controller when this kind of faults occurs.

Remark 7. Several operation points, reference values and perturbations values were simulated, obtaining a good performance for the closed loop system.

5. CONCLUSIONS

In this paper a novel IHOSM control scheme was developed for a wind energy conversion system, to regulate de active power output and PF in the stator of a DFIG, connected to a wind turbine. The mathematical model includes the generator electrical and mechanical dynamics, and the wind turbine behaviour. The control law is presented as a function of the generator voltages and currents, as well as the rotor speed, which can be measured directly, in such a way that an observer is not required. The closed-loop system stability analysis was carried out to show the controller stability properties. The interconnections of the DFIG with the EPS are included in the mathematical model, and the proposed IHOSM control scheme can be implemented in any kind of EPS, with other generators, transmission lines and loads.

The designed controller was tested through simulation under the most typical perturbations in electric power systems, such that generator parameters variations, disturbances of mechanical torque, variations of the interconnection voltage and three phase short circuits in terminals of the DFIG. The simulation results show that the proposed IHOSM control scheme guarantee the regulation of the active power and PF

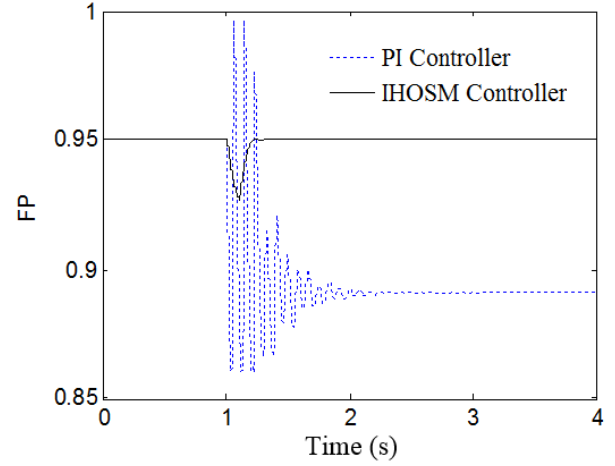in the stator of the generator, under small and large disturbances.

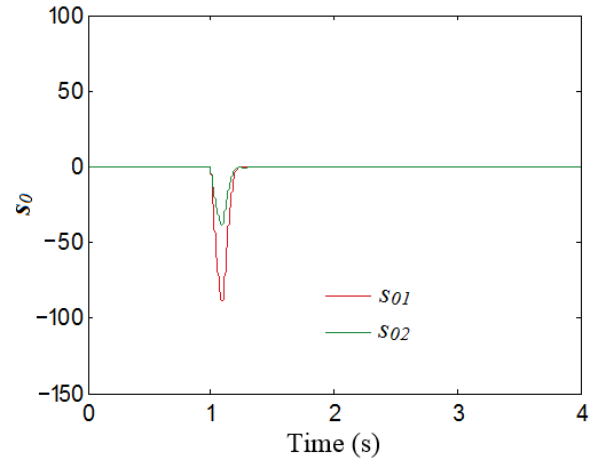Fig. 13. Power factor under perturbation d).

Fig. 14. Sliding manifold convergence under perturbation d).

NOMENCLATURE

α	Constant parameter of the mathematical model.
β	Blade tip pitch angle.
$C_p(\gamma, \beta)$	Power coefficient.
γ	Tip speed ratio.
γ_i	Tip speed relationship.
e	Control error vector.
G	Transmission rate.
$g(I_{dq}, V_{dq}, T_m)$	Perturbation vector.
$g_s(I_{dq}, V_{dqs}, T_m)$	Stator perturbation vector.
$g_r(I_{dq}, V_{dqs}, T_m)$	Rotor perturbation vector.
$g_{PQ}(I_{dq}, V_{dqs}, T_m)$	Perturbation term in the error dynamics equation.
I_{dq}	Currents vector.
I_{dqs}, I_{dqr}	Stator and rotor currents vectors.
I_{ds}, I_{qs}	Direct and quadrature stator axis currents.
I_{dr}, I_{qr}	Direct and quadrature rotor axis currents.
IHOSM	Integral High Order Sliding Modes.
ISM	Integral Sliding Modes.
J	Rotor inertia constant.

k_1, $k_{0,1}$, $k_{0,2}$	Control scheme parameters.
L_s, L_r, L_m	Stator, rotor and mutual inductances.
n_p	Pole pair number.
P	Stator active power output.
P_{ref}	Stator active power output reference.
PF	Stator power factor.
PF_{ref}	Stator power factor reference value.
$\boldsymbol{PQ}$	Stator power output vector.
$\boldsymbol{PQ_{ref}}$	Stator power output references vector.
P_{wt}	Power output of the wind turbine.
Q	Stator reactive power.
Q_{ref}	Stator reactive power output reference.
R	Rotor diameter.
r_s, r_r	Stator and rotor winding resistances.
ρ	Air density.
$\boldsymbol{s_1}$	Integral sliding manifold vector.
$\boldsymbol{s_0}$	Sliding manifold vector.
$\boldsymbol{\sigma}$	Integral vector.
T_e	Electromagnetical torque.
T_m	Mechanical torque.
T_{wt}	Wind turbine mechanical torque.
$\boldsymbol{V_{dq}}$	Voltages vector.
$\boldsymbol{V_{dqs}}$, $\boldsymbol{V_{dqr}}$	Stator and rotor voltages vectors.
V_{ds}, V_{qs}	Direct and quadrature stator axis voltages.
V_{dr}, V_{qr}	Direct and quadrature rotor axis voltages.
$\boldsymbol{V_{dqr,0}}$	Nominal part of the control input.
$\boldsymbol{V_{dqr,1}}$	Perturbation rejection part of the control input.
$\boldsymbol{V_{dqr,1eq}}$	Equivalent control.
v_w	Wind speed.
ω_b	Stator electrical speed.
ω_r	Rotor speed.
ω_s	Stator magnetic field speed.
ω_t	Wind turbine angular speed.
X_{ls}, X_{lr}, X_m	Stator, rotor and mutual reactances.

ACKNOWLEDGEMENTS

REFERENCES

Abdeddaim, S. and Betka, A. (2013). Optimal tracking and robust power control of the DFIG wind turbine, *Electric Power Energy Systems*, 49, 234 – 242.

Anderson, P. M. and Fouad, A. (1994). Power System Control and Stability, *Prentice Hall*, New York, USA.

Belkaid, A., Gaubert, J. and Gherbi, A. (2016). An improved sliding mode control for maximum power point tracking in photovoltaic systems, *Control Engineering and Applied Informatics*, 18(1), 86–94.

Burlibasa, A., Munteanu, I. and Bratcu, A. (2012). Control law design of a low-power wind energy system using active speed stall techniques, *Control Engineering and Applied Informatics*, 14(3), 15–24.

Castillo B., Di Gennaro, S., Loukianov, A. G. and Rivera, J. (2007). Robust Nested Sliding Mode Regulation with Application to Induction Motors, *Proceedings of the American Control Conference*, New York, USA, July 11-13, 2017, pp. 5242-5247.

Datta, R. and Ranganathan, V. T. (2002). Variable-speed wind power generation using doubly fed wound rotor induction machine-a comparison with alternative schemes, *IEEE Transactions on Energy Conversion*, 17(3), 414 – 421.

Fridman, L. and Levant, A. (1996). Higher order sliding modes as a natural phenomenon in control theory, Springer-Verlag, *New York, Lectures notes Control and Information Science*, 217, 107-133.

Ghedamsi, K. and Aouzellag, D. (2010). Improvement of the performances for wind energy conversions systems. *Electric Power & Energy Systems* 32(9), 936 - 945.

Hachicha, F. and Krichen, L. (2012). Rotor power control in doubly fed induction generator wind turbine under grid faults, *Energy*, 44(1), 853–861.

H. Huerta. (2014). Integral high order sliding modes control of double fed induction generator, *Proc. of Latin American Conference of Automatic Control*, Cancún, México October 2014, 1137-1142.

H. Huerta. (2016). Energy-based robust control of doubly-fed induction generator, *Iranian Journal of Science and Technology, Transactions of Electrical Engineering*, 40 (1), 23-33.

Iacchetti, M. F., Marques, G. D., and Perini, R. (2014). Operation and design issues of a doubly fed induction generator stator connected to a dc net by a diode rectifier, *IET Electric Power Applications*, 8(8), 310-319.

Jafari, S. H., Raoofat, M. and Samet, H. (2014). Improving transient stability of double fed induction generator using fuzzy controller. *International Transactions on Electrical Energy Systems*, 24(8): 1065-1075.

Javan, E., Darabi, A., Gharofi, H. M. and Emami, A. (2013). Improved control of DFIG using stator-voltage oriented frame under unbalanced grid voltage conditions. *International Transactions on Electrical Energy Systems*, 23(6), 767-783.

Jazaeri, M. and Samadi, A. A. (2015). Self-tuning fuzzy PI-based controller of DFIG wind turbine for transient conditions enhancement. *International Transactions on Electrical Energy Systems*, 25(11): 2657-2673.

Jiabing, H. and Yikang, H., (2009) Modeling and enhanced control of DFIG under unbalanced grid voltage, *Electric Power Systems Research*, 79(2): 273 - 281.

Kassem, A., Hasaneen, K., and Yousef, A. (2013). Dynamic modeling and robust power control of DFIG driven by wind turbine at infinite grid, *Electric Power & Energy Systems*, 44, 375-382.

Khalil, H. K. (1996). Nonlinear systems, *Prentice Hall, Inc. Simon and Schuster*, New Jersey, USA.

Krause, P. C., Wasyncsuk, O. and Sudhoff, S. D. (2002). Analysis of Electric Machinery and Drive systems, *Jhon Wiley and Sons*, New York, USA.

Lee, S., Lee, K, Lee D., and Kim, J., (2010). An improved control method for a DFIG in a wind turbine under an unbalanced grid voltage condition. *Journal of Electrical Engineering & Technology*, 5(4), 614–622.

Leon, A. E., Mauricio, J. M. and Solsona, J. A. (2012). Fault ride-through enhancement of DFIG-based wind

generation considering unbalanced and distorted conditions, *IEEE Transactions on Energy Conversion*, 27(3),775 - 783.

Mansour, M., Mohammad, M. and Syed, I. (2011). Low and high voltage ride-through of DFIG wind turbines using hybrid current controlled converters, *Electric Power Systems Research*, 81(7), 1456 - 1465.

Marchi, D. A., Dainez, P. S., Von Zuben, F. J. and Bim, E. (2014). A multilayer perceptron controller applied to the direct power control of a doubly fed induction generator, *IEEE Transactions on Sustainable Energy*, 5(2): 498-506.

Moreno, J. and Osorio, M. (2008). A Lyapunov approach to second-order sliding mode controllers and observers, *Proceedings of the 47th IEEE Control Decision Conference*.

Morfin, A., Ruiz-Cruz, R., Loukianov, A. G., Sanchez, E. N., Castellanos, M. I. and Valenzuela F. A. (2014). Torque controller of a doubly-fed induction generator impelled by a DC motor for wind system applications, *IET Renewable Power Generation*, 8, 484 - 497.

Patnaik, R. K., Dash, P. K. and Mahapatra, K. (2016). Adaptive terminal sliding mode power control of DFIG based wind energy conversion system for stability enhancement. *International Transactions on Electrical Energy Systems*, 26(4), 750 – 782.

Rahim, A. H. and Habiballah, I. O. (2011). DFIG rotor voltage control for system dynamic performance enhancement, *Electric Power Systems Research*, 81(2), 503 – 509.

Rossomando, F., Soria. C. and Carelli, R. (2014). Sliding mode control for trajectory tracking of a non-holonomic mobile robot using adaptive neural networks, *Control Engineering and Applied Informatics*, 16(1), 12–21.

Song, H. H. and Qu, Y. B. (2013). Energy-based excitation control of doubly-fed induction wind generator for optimum wind energy capture. *Wind Energy* 2013; 16(5): 645-659.

Utkin, I., Guldner, J. and Shi, J. (1999). Sliding Mode Control in Electromechanical Systems, *Taylor & Francis, London.*

Wang, H., Pintea, A., and Christov, N. (2012). Modelling and recursive power control of horizontal variable speed wind turbines, *Control Engineering and Applied Informatics*, 14(4), 33–41.

Zarei, M. E. and Asaei, B (2016). A robust direct current control of DFIG wind turbine with low current THD based predictive approach. *Wind Energy*, 19(7), 1181-119